Feasibility study of the photonuclear reaction cross section of medical radioisotopes using a laser Compton scattering gamma source*

Yu-Ning Gu,[1,2,3] Wei-Juan Zhao,[1] Xi-Guang Cao,[2,3,4,†] Yu-Xuan Yang,[1,3]
Tin-Kai Ma,[2,3,5] Zheng-Li Liao,[3,4] Fei-Long Xu,[3,4] and Yu-Gang Ma[6,7]

[1]*School of Physics and Microeletronics, Zhengzhou University, Zhengzhou 450001, China*
[2]*Shanghai Advanced Research Institute, Chinese Academy of Sciences, Shanghai 201210, China*
[3]*Shanghai Institute of Applied Physics, Chinese Academy of Sciences, Shanghai 201800, China*
[4]*University of Chinese Academy of Sciences, Beijing 100049, China*
[5]*School of Nuclear Science and Technology, University of South China, 421001 Hengyang, China*
[6]*Key Laboratory of Nuclear Physics and Ion-beam Application (MOE), Institute of Modern Physics, Fudan University, Shanghai 200433, China*
[7]*Shanghai Research Center for Theoretical Nuclear Physics, NSFC and Fudan University, Shanghai 200438, China*

In recent years, the gap between the supply and demand of medical radioisotopes has increased, necessitating new methods for producing medical radioisotopes. Photonuclear reactions based on gamma sources have unique advantages in terms of producing high specific activity and innovative medical radioisotopes. However, the lack of experimental data on reaction cross sections for photonuclear reactions of medical radioisotopes of interest has severely limited the development and production of photonuclear transmutation medical radioisotopes. In this study, the entire process of the generation, decay, and measurement of medical radioisotopes was simulated using online gamma activation and offline gamma measurements combined with a shielding gamma-ray spectrometer. Based on a quasi-monochromatic gamma beam from the Shanghai Laser Electron Gamma Source (SLEGS), the feasibility of the measurement of production cross section for surveyed medical isotopes was simulated, and specific solutions for measuring medical radioisotopes with low production cross sections were provided. The feasibility of this method for high precision measurements of the reaction cross section of medical radioisotopes was demonstrated.

Keywords: Medical radioisotope; Photonuclear reaction; GEANT4; Shanghai Laser Electron Gamma Source (SLEGS); low-background gamma-ray spectrometer

I. INTRODUCTION

In recent years, the shortage of medical radioisotopes has been repeatedly highlighted[1, 2], and the gap between the supply and demand of medical radioisotopes has become increasingly prominent. Currently, the global production of medical radioisotopes is concentrated in a few large research reactors with a global supply strategy. These include the National Research Universal Reactor in Canada, High Flux Reactor in the Netherlands, High Flux Isotope Reactor in the United States, and Missouri University Research Reactor in the United States. However, the specific activity of the medical radioisotopes produced by reactors is low, and the aging reactors built in the 1950s and the 1960s are being decommissioned. Therefore, a new methods for producing medical radioisotopes with higher specific activity are urgently required[3].

Photonuclear reactions have attracted considerable attention worldwide because of their good selectivity, relatively single reaction products, and high specific activity of the radioisotopes produced by photonuclear transmutation. The reports of the Nuclear Science Advisory Committee-Isotope Subcommittee in 2009 and 2015 concluded that the study of radioisotope production methods based on accelerators was essential and the photonuclear transmutation method based on an electron linear accelerator was a unique source of radioisotopes [4, 5]. Recently, the Nuclear Science Advisory Committee described this approach as one of the most compelling and influential opportunities for producing medical radioisotopes with high specific activity.

Two methods for photonuclear transmutation exist. One method uses an electron accelerator to generate bremsstrahlung to drive photonuclear transmutation [6]. The second method is based on photonuclear transmutation driven directly by the next generation of quasi-monochromatic gamma sources [7]. However, regardless of the approach, the greatest uncertainty arises from the cross section of the photonuclear reaction. For most known medical radioisotopes that can be produced, as well as innovative medical radioisotopes with significant potential applications, the scarcity of data on the reaction cross section of photonuclear reactions severely limits the study and development of medical radioisotopes produced by photonuclear reactions

* Supported by the Strategic Priority Research Program of the CAS (No. XDB34030000), National Natural Science Foundation (No. 11975210, No. U1832129), National Key Research and Development Program of China (No. 2022YFA1602404), and Youth Innovation Promotion Association CAS (No. 2017309)

† Corresponding author, CAO xiguang, Email:caoxg@sari.ac.cn

and the evaluation of photonuclear transmutation efficiency and selection of target nuclear reaction paths. In the electron-accelerator-driven scheme, the photonuclear reaction cross section determines the selection of the highest energy of the electron accelerator, which affects the maximum yield of the target isotope and specific activity of the product. Furthermore, the photonuclear reaction cross section affects the energy selection of the quasi-monochromatic gamma source and the assessment of the specific activity of the product. Therefore, measuring the photonuclear reaction cross section for medical radioisotopes of interest is highly significant.

High-precision measurements of the reaction cross section can be performed by offline measurements with shielding devices, which reduce interference from the surrounding environment gamma, neutron, and cosmic rays and improve the signal-to-noise ratio, even when the characteristic gamma intensity branching ratio is small. In our simulation, a quasi-monochromatic gamma beam was used to activate the target material, and the characteristic gamma rays of radioisotopes produced by photonuclear reactions were measured with an offline measuring device to detect the types and quantities of target nuclides generated in the reactive target. Finally, the reaction cross sections of photonuclear reactions (γ, n), (γ, p), and (γ, γ') were obtained. A low-background gamma-ray spectrometer was used to obtain high-precision reaction cross sectional measurements. Based on the quasi-monochromatic gamma beam of the Shanghai Laser Electron Gamma Source (SLEGS) [8, 9], the entire process of medical isotope production, decay, and measurement was simulated using the GEANT4 toolkit [10–12]. Finally, the feasibility of medical radioisotopes of interest is discussed. This study is of guiding significance for measuring reaction cross sections of medical radioisotopes produced by photonuclear reactions.

II. MEASUREMENT METHOD

The parameters for the candidate medical radioisotopes produced by the (γ,n) and (γ,p) reactions are listed in Table 1 [13–15]. The theoretical reaction cross section data in the energy region are obtained from the TENDL-2021 database. Most photonuclear reaction cross sections for medical radioisotopes of interest in the giant dipole resonance energy region do not have experimental data and require further accurate measurements through experiments.

Generally, two methods are used to measure the reaction cross section of the (γ, n), (γ, p), and (γ, γ') reactions that generate target nuclei: the first directly measures the neutron, proton, and γ' products generated by the reaction online, while the second performs offline measurements of the characteristic gamma rays of the target nucleus produced by the online activation. However, natural targets typically contain multiple isotopes, making it impossible to distinguish which isotope the neutrons, protons, and γ products detected by online measurements originated from. Furthermore, achieving 100% purity is difficult even with enriched isotopic targets, and accurate measurements of reaction cross sections with high-purity isotopic targets are expensive. The measurement of small reaction cross sections is difficult owing to the background from bremsstrahlung radiation in the gamma beam and natural background from the environment.

Table 1. Information on several medical radioisotopes in the region of interest.

Isotope	Reaction Channel	Half-life	Decay Modes	γEnergy MeV	Cross Section mb	$E_\gamma(I_\gamma)$ keV(%)
^{186}Re	^{187}Re(γ,n)^{186}Re	3.72 d	$\beta^- = 92.53\%$	13.5	365.579	137.157(9.47)
^{68}Ga	^{69}Ga(γ,n)^{68}Ga	67.71 m	$\varepsilon = 100.00\%$	16.5	109.096	1077.34(3.22)
^{67}Cu	^{68}Zn(γ,p)^{67}Cu	61.83 h	$\beta^- = 100.00\%$	19.5	1.984	184.577(48.7)
^{47}Sc	^{48}Ti(γ,p)^{47}Sc	3.35 d	$\beta^- = 100.00\%$	21	11.848	159.381(68.3)
^{64}Cu	^{65}Cu(γ,n)^{64}Cu	12.701 h	$\varepsilon = 61.50\%$	17	84.72	1345.77(0.47)
			$\beta^- = 38.50\%$			

Compared to direct online measurements, offline measurements completely separate the activity measurement of radionuclides from the photonuclear excitation process and effectively avoid interference from low-energy neutrons, X/γ rays of various energies, and the positron pair spectrum caused by online irradiation [16–18]. Moreover, medical radioisotopes typically have long half-lives and emit gamma rays during decay, making offline decay measurements well-suited. However, most medical radioisotopes possess relatively small photonuclear reaction cross sections. Typically, the characteristic peaks of the γ spectrum of photonuclear activation products in the irradiated target material measured offline are submerged in the environmental background. Thus, the detection limit depends on the background level.

Low-background gamma ray spectroscopy with germanium (Ge) detectors has become a fundamental tool for identifying and measuring the activity of radionuclides in samples, determining the emission probabilities of radioactive decay, and conducting low-level counts [19].

Table 2 presents a survey of reported low-background systems. All the systems possess an integrated background of $\leq 0.12\,\mathrm{c/s/100cm^3Ge}$ [20–25]. Additionally, if only passive material shielding is considered, the integrated background can reach a level below $2\,\mathrm{c/s}$ under better conditions. Therefore, a low-background gamma-ray spectrometer for offline measurements

of medical radioisotopes has been proposed, which reduces the background, achieves high-precision measurements of reaction cross sections, reduces the irradiation time, and saves valuable beam time.

Table 2. Survey of reported low-background γ spectrometry systems.

Active shielding	Energy range keV	Integrated background $\mathrm{c/s/100cm^3Ge}$	Reference
Plastic scintillator	$100 \sim 2000$	4.1×10^{-2}	Miley H S, et al.(1992)
4-sided plastic scintillator	$50 \sim 3000$	1.2×10^{-1}	Byun J I, et al.(2003)
6-sided plastic scintillator	$100 \sim 2000$	2.5×10^{-2}	Diao L J, et al. (2010)
12-sided plastic scintillator	$40 \sim 2700$	2.1×10^{-3}	Heusser G, et al.(2015)
9-sided plastic scintillator	$40 \sim 2700$	4.9×10^{-2}	Hu Q D, et al. (2016)

The target nuclei produced by online irradiation can be identified by their characteristic gamma energies and half-lives. N_0 is the number of target nuclei obtained at the end of irradiation, and N is the integral count of the gamma full-energy peak.

$$N = N_0 I_\gamma \epsilon_\gamma C_{k\gamma} e^{-\lambda t_d}(1 - e^{-\lambda t_m}), \tag{1}$$

where I_γ is the gamma decay intensity obtained from the NNDC database, ϵ_γ is the detection efficiency of HPGe, which can be calibrated using a gamma standard source with known intensity; $C_{k\gamma} = e^{-(\mu/\rho)\rho x}$ is the penetration factor of gamma-ray of target nuclear decay; μ/ρ is the mass attenuation coefficient$(\mathrm{cm^2/g})$; ρx is the mass thickness of the target$(\mathrm{g/cm^2})$; λ is the decay constant of the target nucleus; t_d is the time interval between the end of irradiation and the start of measurement; and t_m is the time of offline measurement. As a general activation measurement [26],

$$N_0 = \sigma(E) N_t Q C_{kbeam} \int_0^{t_i} \varphi(t) e^{-\lambda t} dt, \tag{2}$$

where $\sigma(E)$ is the energy dependent reaction cross section; N_t is the surface density of the target nucleus $(\mathrm{atoms/cm^2})$; Q is the abundance of the target isotope in the target; C_{kbeam} is the penetration factor of the incident gamma beam in the target; $\varphi(t)$ is the γ beam intensity as a function of time; and t_i is the irradiation duration. If $\varphi(t)$ is approximated as a constant, then

$$N_0 = \frac{\sigma(E)\phi N_t Q C_{kbeam}(1 - e^{-\lambda t})}{\lambda}, \tag{3}$$

where ϕ is the integrated gamma-ray flux; Because N_0 can be measured from N using Eq. (1), the reaction cross section can be obtained from Eq. (2). The gamma flux from the real measurement of SLEGS was found to be stable because of the stable electron beam intensity of the SSRF storage ring and the laser beam used for Compton scattering. A specific form of the beam intensity $\varphi(t)$ was required to perform the simulation. A constant beam-intensity approximation was used to study the feasibility of cross-sectional measurements based on realistic beam-intensity measurements. After determining the measurement method for the photonuclear reaction cross section, a low-background gamma spectrometer was constructed using GEANT4 and the feasibility of the method was assessed by simulating the entire process of photonuclear reactions for producing medical radioisotopes and offline measurements.

III. SIMULATION MODELING

GEANT4 is a Monte Carlo simulation toolkit, which is widely used in particle physics, astrophysics, nuclear physics, medical physics, radiation protection, and other fields [12]. GEANT4 enables accurate numerical simulations of interactions between matter and particles, including particle transport, energy deposition, electromagnetic interactions, and nuclear reactions. It also supports extensions in various aspects, such as particle type, geometry, material properties, detector type, and computer operating systems. The main advantages of GEANT4 are its high reproducibility and reliability. Based on GEANT4, we developed a program for simulating medical isotope production, decay, and measurement and performed full-scale simulations.

A. Medical isotope production

A Laser Compton Scattering (LCS) light source is a new X-ray or Gamma-ray source based on the interaction of a relativistic electron beam with laser photons. It is characterized by high energy, short wavelength, fast pulses, and high peak brightness,

and has become an important option for advanced international light source technology [27]. SLEGS) produces gamma rays in the energy range of 0.4–20 MeV, thereby covering the energy range from the nuclear structure to giant resonance (keV to MeV) in nuclear physics research. The gamma ray flux integrated over the entire spectrum can reach 10^5-10^7 phs/s and is continuously adjustable. Collimation technology can be used to achieve an energy spread greater than 5% [8, 28]. Therefore, in our simulation, we used a gamma beam with an intensity and energy spread of 10^7 phs/s and of 5%, respectively, to activate the Ti target and produce the target medical isotope, ^{47}Sc, via the ^{48}Ti(γ,p)^{47}Sc reaction for further analysis.

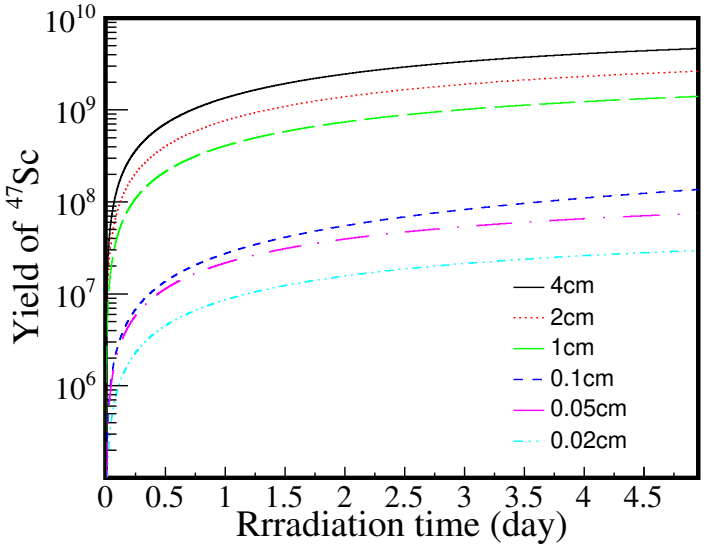

Fig. 1. Variation of the yield of ^{47}Sc with irradiation time for targets of different thicknesses.

Fig. 1 shows that within the first half day of irradiation, the yield of ^{47}Sc increases rapidly, and after the irradiation time exceeds half a day, the yield gradually approaches a saturation value of one. The choice of the target thickness was related to the penetration factor of the incident gamma beam in the target(C_{kbeam}). As the thickness of the target increased, the photons needed to penetrate a longer distance through the target material, resulting in a decreased photon count. Simultaneously, multiple scattering inside the target produced a broader distribution of photon energies. In addition, the choice of the target thickness was also related to the penetration factor of the gamma rays produced by the target nucleus decay ($C_{k\gamma}$). The gamma rays produced by the decay of the target nucleus attenuated with increasing thickness of the target, and the integral count of the gamma full-energy peak decreased, which affected the measurement.

B. Low-background gamma-ray spectrometer

The significant effect of the background radiation on the measured energy spectrum results in unreliable analytical results. Background radiation primarily originates from three sources: natural environmental radiation from the laboratory environment, radioactive background from the detection components and shielding materials, and cosmic ray contributions. Low-background gamma spectrometers must be shielded against background radiation to achieve high-precision reaction cross section measurements of medical radioisotopes.

Many low-background gamma-ray spectrometers have been constructed domestically and internationally. Moreover, countries such as China, France, the United States, and Japan have established underground laboratories at different depths to facilitate research in low-background measurement fields. Representative devices abroad include those of the same type established by Miley at thePacific Naval Laboratory in 1991 [20], Byun at the Korea Atomic Energy Research Institute in 2001 [21], Semkow et al. in the United States in 2002 [19], and Heusser et al. in Germany [23, 24]. Such devices have also been built in laboratories in China, including the China Institute of Atomic Energy [22], Institute of High Energy Physics of the Chinese Academy of Sciences, and Third Institute of Oceanography of the State Oceanic Administration [25].

Based on existing low-background gamma spectrometers, a low-background gamma spectrometer was designed using GEANT4 simulations to achieve a shielding effect. The shielding structure is illustrated in Fig. 2 [29].

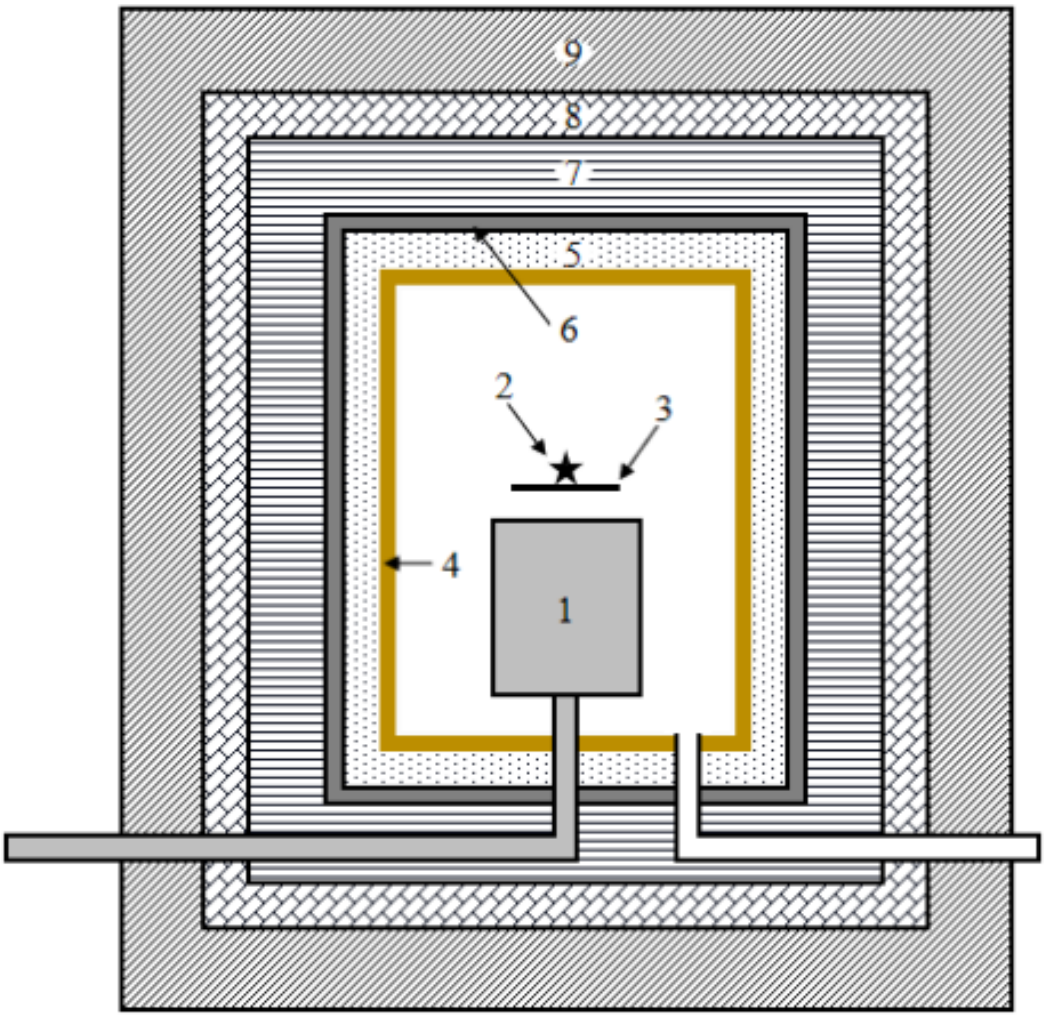

Fig. 2. Low-background gamma-ray spectroscopy with shielding structure:1.HPGe detector, 2.sample to be measured, 3.plastic holder, 4.the copper liner(2 mm-thick), 5.inner lead(50 mm-thick), 6. cadmium absorber(3 mm-thick), 7.borated polyethylene(100 mm-thick), 8.plastic scintillator(50 mm-thick), 9.outer lead(100 mm-thick).

Using a high-purity germanium detector for a low-background gamma spectrometer requires careful consideration of shielding from various backgrounds. The gamma ray intensity decreases drastically as the atomic number of the material increases because materials with higher atomic numbers possess larger gamma attenuation factors than those with lower atomic numbers [30, 31]. Common high-Z materials include lead, oxygen-free copper, and steel; however, iron is easily contaminated with ^{60}Co during smelting, and copper has a large thermal neutron capture reaction cross section. Considering factors such as the price, atomic number, and mechanical properties, lead is the best choice for gamma shielding materials.

Cosmic rays in the environment produce secondary particles, such as photons, neutrons, and electrons, when they undergo muon capture in materials with large atomic numbers, such as lead [32–36]. Therefore, the second layer of the shielding device considers neutron shielding. Neutrons must undergo deceleration and absorption. Water, paraffin, and polyethylene are widely used as slowing down materials [37]. Plastic scintillators or polyethylene can be used as a second layer to slow down fast neutrons.

The third layer is used to absorb thermal neutrons. ^{10}B is an excellent absorber of thermal neutrons and B_4C has a B/C ratio of 0.7828, resulting in a very large neutron capture reaction cross section. Thus, it can effectively absorb decelerated neutrons. Additionally, cadmium has a large absorption reaction cross section for thermal neutrons. Therefore, boron-containing polyethylene can be used to slow down and absorb neutrons, whereas cadmium can be used to absorb thermal neutrons [38]. However, cadmium atoms emit gamma rays with an energy of 2.3 MeV after capturing neutrons. Therefore, a low-background lead must shield this portion of the gamma rays.

Finally, other low-Z materials, such as organic glass or copper, can be added to the inner lining to shield against impurities, such as ^{210}Pb, its daughter nucleus ^{210}Bi in lead, and the characteristic X-rays of lead [39]. The shielding structure was determined through simulations to select appropriate shielding materials and optimize their thicknesses. The final shield structure from the outside to the inside was determined to be:100 mm thick lead, 50 mm thick plastic scintillation, 100 mm thick borated polyethylene, 3 mm thick cadmium, 50 mm thick lead, and 2 mm thick oxygen-free copper, which was consistent with the low-background gamma spectrometer designed by Hu et al. [25].

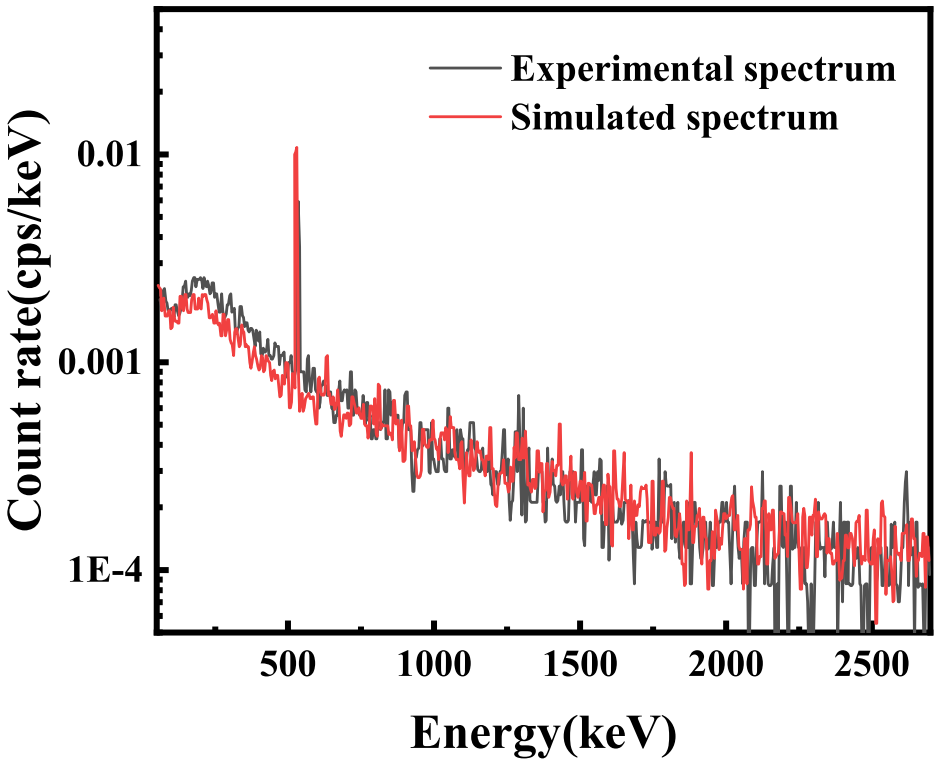

Fig. 3. Comparison between the simulated and experimental spectra.

In Fig. 3, a comparison of the simulated HPGe energy deposition spectrum with the results obtained by Hu et al., reveals a similar trend, and the count rate of the 511 keV peak in the spectrum possesses the same order of magnitude (approximately 8×10^{-3} cps). It is essential to note that because of the shielding configuration employed, specifically the incorporation of an inner lead layer in our shielding system, the 478 keV peak is obscured and consequently, not evident in Fig. 3. In the low-energy range, the count rate of the experimental spectrum exceeds that of the simulated spectrum owing to the differences in the background and radioactivity of the shielding material and detector. Thus, the reliability of the simulations was verified.

C. Medical isotope decay and measurement

Based on the passive-shielding conditions shown in Fig. 2, the total integral background count rate in the energy range of 100∼2700 keV obtained by the simulation is $0.22\,\mathrm{c/s/100cm^3Ge}$, whereas under the better condition of using only lead shielding, the total integral background count rate in the energy range of 100∼2700 keV may reach 1 cps [25, 40, 41]. To reduce simulation complexity, we used lead shielding only in the following simulation. Based on the spectrometer constructed in the GEANT4 simulation program, the number of target nuclei ^{47}Sc produced was considered as the input for offline decay measurement simulation when the offline measurements lasted for only 1 h and only lead shielding was used.

In Fig. 4, we present the spectra obtained by simulations under different conditions(Shanghai electron laser gamma source laboratory environment background, low background shielding device, and neglecting the environmental background). After background subtraction, the integral count rate of the gamma full-energy peak from the decay of ^{47}Sc is $0.16\,\mathrm{c/s}$ at E_γ= 159 keV. When measured in the environmental background, the gamma full-energy peak of ^{47}Sc is completely submerged in the background. Low-background shielding effectively reduced the lower limit of detection was, and the integral count of the gamma full-energy peak of the characteristic peak was identifiable.

Therefore, the cross sections for medical radioisotopes produced by photonuclear reactions were efficiently measured by

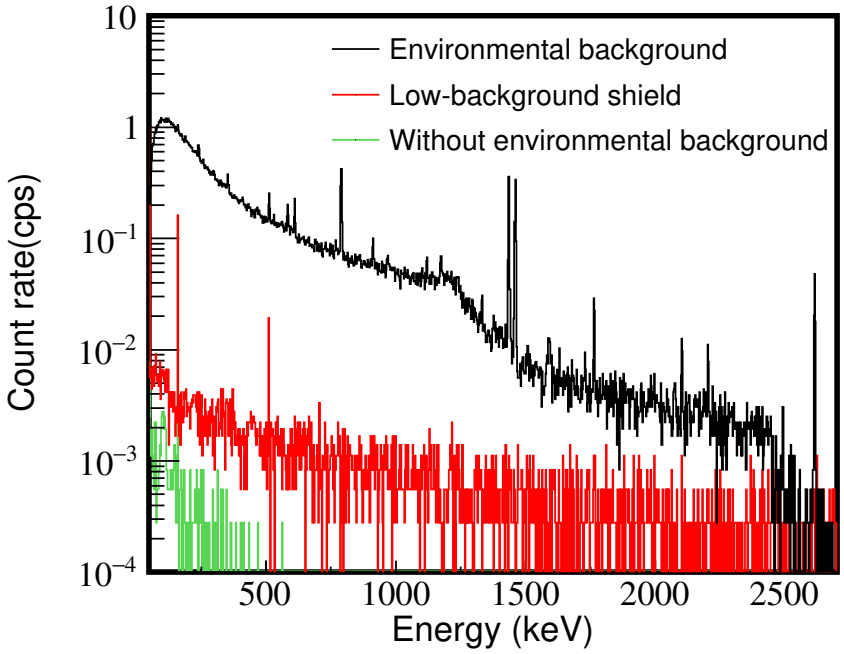

Fig. 4. Simulated spectra of ^{47}Sc under different conditions.

reducing the background. In addition, factors such as the irradiation time, measurement time, and beam intensity affected cross section measurements. In the next section, we discuss the detection lower limit through computational simulations.

IV. FEASIBILITY OF MEASUREMENT

Our simulation program includes five control parameters: irradiation time, measurement time, time interval between the end of the irradiation and the beginning of the measurement, thickness of the target, and beam intensity. Considering the influence of the background in a real environment, the background was considered as the sixth control parameter. Based on SLEGS, the gamma beam intensity factor can be set to 10^7 phs/s [8].

First, we considered the background factor. According to Eq. (1), N is the integral count of the gamma full-energy peak when the background is neglected. However, the detector measures the integral count of the gamma full-energy peak produced by the decay of the target nucleus in combination with the background. Therefore, we obtained the following relationship:

$$N = C - C_0, \tag{4}$$

where C and C_0 denote the integral count of the gamma full-energy peak produced by the decay of the target nucleus measured by the detector and the background count by the low-background detection system (considering only lead shielding), respectively. For realistic measurements, the relative statistical error of the counts was set to 10%. According to the error propagation formula, the relative statistical error is expressed by Eq. (5)

$$\upsilon = \frac{\sqrt{C + C_0}}{C - C_0}. \tag{5}$$

Subsequently, the target thickness was considered. According to Eqs. (1) and (2), the thickness of the target mainly affects the attenuation coefficient and area density. We constructed a function $f(x)$ that varies with the thickness of the target, as shown in Eq. (6) as follows:

$$f(x) = N_t C_{k\gamma} C_{kbeam} = \frac{N_A \rho x e^{-(\mu/\rho)\rho x} e^{-(\mu'/\rho)\rho x}}{M}, \quad (6)$$

where $N_t = \frac{N_A \rho x}{M}$, N_A is the Avogadro constant; M is the molar mass; ρx is the mass thickness of the target; μ is the attenuation coefficient of the photon beam incident on the target during online activation; and μ' is the attenuation coefficient of de-excitation gamma escaping the target in offline measurements. Using $^{69}Ga(\gamma, n)^{68}Ga$ as an example, the relationship between $f(x)$ and x is as shown in Fig. 5.

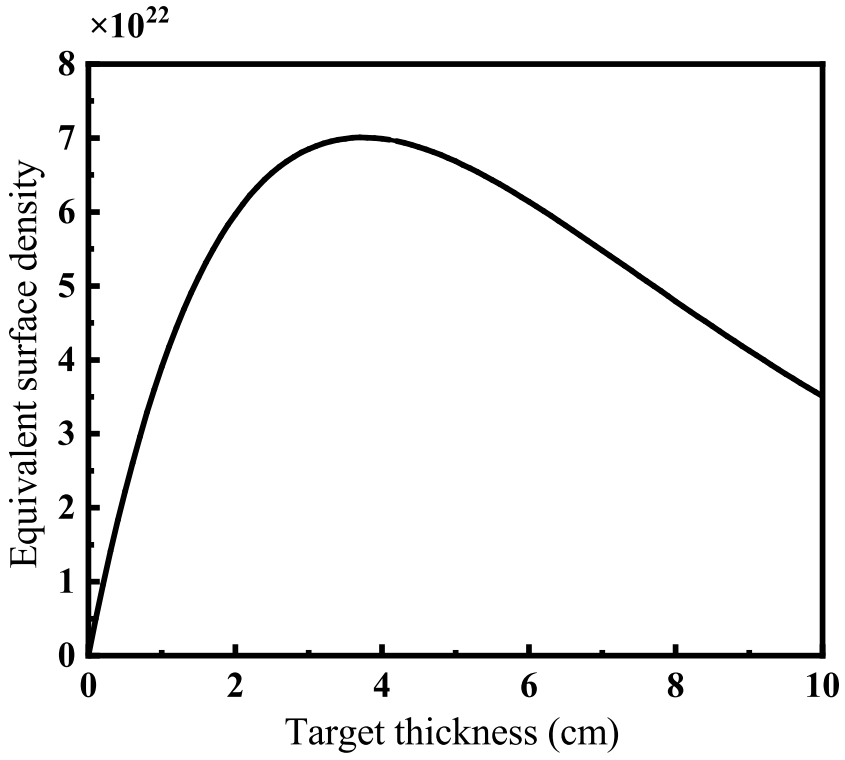

Fig. 5. Dependence of the equivalent surface density on the target thickness for $^{69}\mathrm{Ga}(\gamma, n)^{68}\mathrm{Ga}$

According to Fig. 5, the function $f(x)$ has a maximum value. Rewriting Eqs. (1) and (2) as functions of $f(x)$, as shown in Eq. (7), we obtain:

$$N = \frac{\sigma(E)\phi Q I_\gamma \epsilon_\gamma e^{-\lambda t_d}(1 - e^{-\lambda t_m})(1 - e^{-\lambda t_i}) f(x)}{\lambda}, \quad (7)$$

where $f(x)$ is proportional to N. The maximum integral count N can be determined using $f(x)$ when the other conditions are fixed. In realistic measurements, the thickness of the target nucleus affects the count rate of the characteristic gamma owing to the inevitable attenuation of the gamma incident on the target nucleus and the self-absorption of the target nucleus during deexcitation. Therefore, the thickness must be determined based on practical considerations among other factors. For thicknesses ranging from zero to the optimal value, $f(x)$ increased monotonically with x. Based on this property, the detection limit can be determined by combining time factors.

The time factors include the irradiation time t_i, measurement time t_m, and time interval from the end of irradiation to the beginning of measurement t_d. Here, t_d was uniformly set to 5 min, and the relationship between t_i and t_m was determined from Eq. (7). In other words, when the other conditions were fixed, one quantity increased whereas the other decreased. One can define A = $t_i t_m$. Considering the decay of the target nucleus, t_m is limited to 900-3600 s, and t_i was limited to within 24 h in a realistic case.

Three limiting factors: x, t_m, and t_i were considered. When x had a minimum value of 0.01 cm, offline measurements were used to measure the cross section of medical radioisotopes generated by photonuclear reactions with a 0.01 cm thick target if the simulated values of t_m and t_i were within their respective limits (i.e., t_m was between 900-3600 s and t_i was within 24 h). Measurements were easier for smaller values of A because less time was required for irradiation and measurement. If t_m and t_i were outside their respective limits when x was set to 0.01 cm, the measurement of medical radioisotopes generated by photonuclear reactions was not feasible at this thickness. The detection limit was determined by gradually increasing the thickness in steps of 0.01 cm, and the difficulty in detection was indicated by the values of x and A.

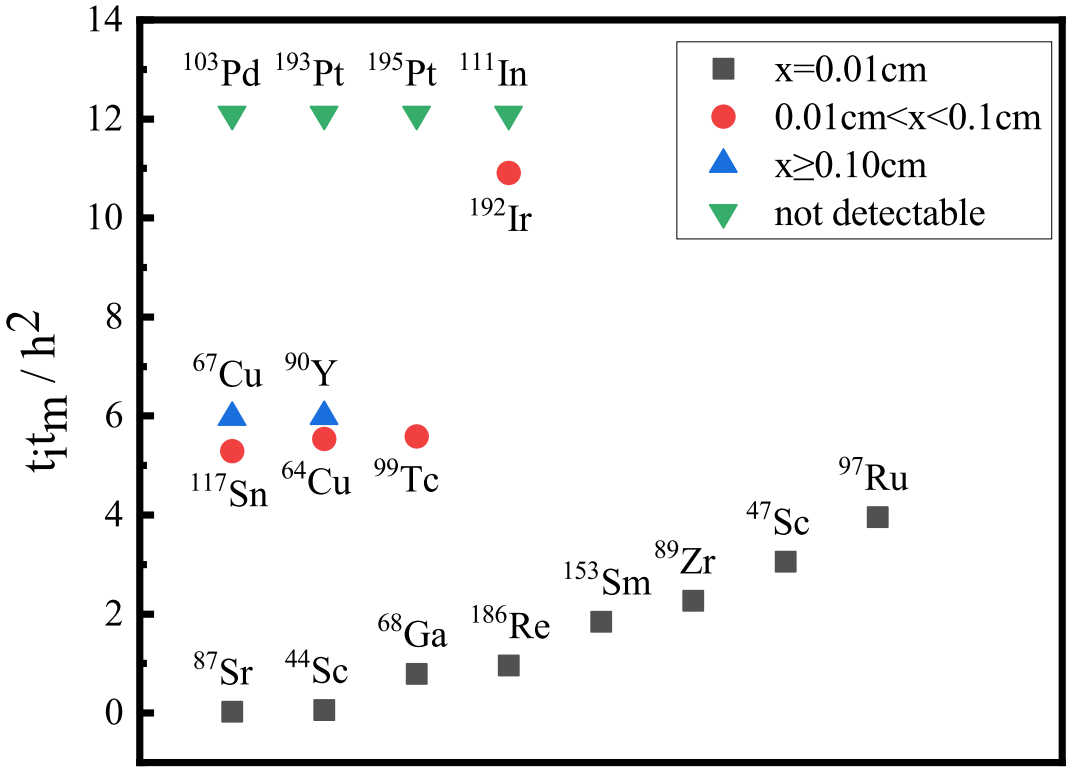

Fig. 6. Feasibility of reaction cross section measurement for some medical radioisotopes, where t_m, t_i, and h represent the time of offline measurement, irradiation duration, and unit of time in hour, respectively.

Some medical radioisotopes of interest were selected, and the simulation was performed using the aforementioned method; the results are shown in Fig. 6. When x = 0.01 cm, ^{87}Sr, ^{44}Sc, ^{68}Ga, ^{186}Re, ^{153}Sm, ^{89}Zr, ^{47}Sc, and ^{97}Ru can be used to measure the production reaction cross section. Smaller values of A indicate shorter irradiation and measurement times. However, ^{45}Ti, ^{103}Pd, ^{193}Pt, ^{195}Pt, and ^{111}In could not be measured within an irradiation time of 24 h and a detection time of 3600 s, even with the optimal thickness.

Several methods can be used to enhance the measurement of reaction cross sections for these medical radioisotopes, such as transferring to stack targets, switching to enriched isotopic targets, increasing the intensity of the gamma beam, and using low-background gamma spectrometers with better shielding.

The characteristic gamma decay can be reduced by stacking several targets together to form a stacked target. Compared to other methods, its implementation is easy. Taking ^{112}Sn(γ,p)^{111}In as an example, natural and stack targets were used for the simulation. The thicknesses of the natural and stack targets were assigned the same value (1 mm) to allow easy comparison of the results. Thus, the natural target was 1 mm thick, and the stack target was divided into five pieces, each with a thickness of 0.2 mm. The results of the comparison are presented in Fig. 7.

For the characteristic gamma $E_\gamma = 171.29$ keV, the count rate of the full-energy peak measured using the natural targets was 0.027 c/s whereas the count rate measured using the stack targets was significantly higher than that of the natural targets at 0.039 c/s. However, the low abundance of ^{112}Sn in the Sn target resulted in a low yield of ^{111}In. During the actual measurement, the existence of the background resulted in relative errorυ exceeding 10%, even with the use of a stack target. Therefore, for cross section measurements of ^{112}Sn(γ,p)^{111}In, enriched isotopic targets can be used to improve feasibility. With 100% isotopic targets, the count rate at $E_\gamma = 171.29$ keV can be increased to 2.409 c/s, and the characteristic gamma full-energy peak can be detected under a low background shield, as shown in Fig. 8.

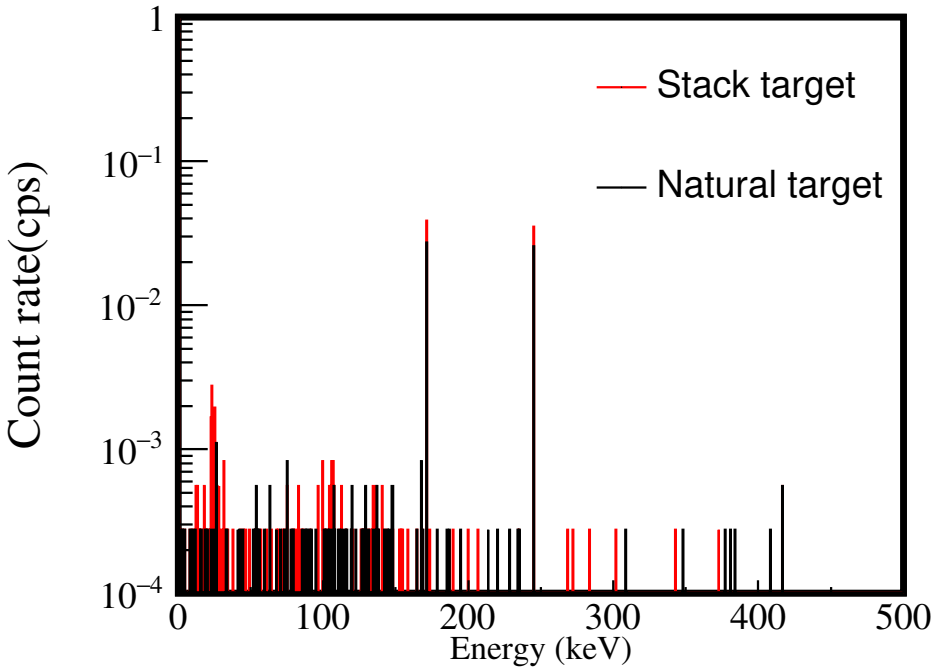

Fig. 7. Comparison of the count rates of the natural and stack targets(^{112}Sn(γ,p)^{111}In).

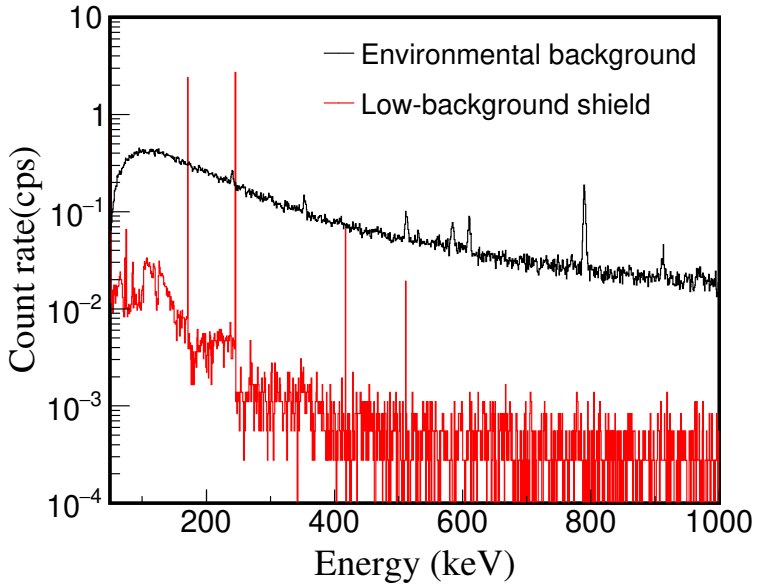

Fig. 8. Decay spectra of ^{111}In under environmental background and low background shield with enriched isotope target.

V. CONCLUSION

Available data on gamma transmutation cross sections for medical radioisotopes are scarce. Measurements of photonuclear reaction cross sections are useful for filling the gaps in data from gamma transmutation experiments, reducing large data errors, and resolving divergences between various theoretical calculations and data. In this study, the generation, decay, and measurement of medical radioisotopes were simulated using GEANT4 combined with a shielding gamma-ray spectrometer. Low background shielding can improve the signal-to-noise ratio, facilitate high-precision measurements, and save the valuable beam time. Based on SLEGS, the feasibility of specific medical radioisotope reaction cross section measurements was presented. SLEGS, the only available gamma facility in China capable of providing intermediate-and high-energy, high-intensity, quasi-monochromatic, energy continuously adjustable gamma beam, is expected to provide an important platform for studying photonuclear reaction cross sections for medical radioisotopes of interest.

VI. ACKNOWLEDGMENTS

We are indebted to Wen-Qing Shen for his significant promotion and helpful suggestions for the study of medical isotopes driven by γ-ray beam transmutation.

[1] P. Gould, Medical isotope shortage reaches crisis level. Nature **460**, 312–313 (2009). doi:10.1038/460312a
[2] R.V. Noorden, Radioisotopes: The medical testing crisis. Nature **504**, 202–204 (2013). doi:10.1038/504202a
[3] Researchers urge action on medical-isotope shortage. Nature **459**, 1045 (2009). doi:10.1038/4591045b
[4] Nuclear Science Advisory Comittee Isotopes Subcommittee, Isotopes for the nation's future—a long range plan, Washington DC, USA, 2009
[5] Nuclear Science Advisory Comittee Isotopes Subcommittee, Meeting Isotope Needs and Capturing Opportunities for the Future, The 2015 Long Range Plan for the DOE-NP Isotope Program, Washington DC, USA, 2015
[6] K.M. Spohr, M. Shaw, W. Galster et al., Study of photo-proton reactions driven by bremsstrahlung radiation of high-intensity laser generated electrons. New j. phys. **10**, 043037 (2008). doi:10.1088/1367-2630/10/4/043037
[7] Y.X. Yang, W.J. Zhao, X.G. Cao et al., Simulation study on the production of medical radioisotopes ^{186g}Re by photonuclear reaction. Radiat. Phys. Chem. **218**, 111599 (2024). doi:10.1016/j.radphyschem.2024.111599
[8] H.W. Wang, G.T. Fan, L.X. Liu et al., Development and prospect of Shanghai laser compton scattering gamma source. Nucl. Phys. Rev. **37**, 53–63 (2020). doi:10.11804/NuclPhysRev.37.2019043 **(in Chinese)**
[9] H.W. Wang, G.T. Fan, L.X. Liu et al., Commissioning of laser electron gamma beamline SLEGS at SSRF. Nucl. Sci. Tech. **33**, 87 (2022). doi:10.1007/s41365-022-01076-0
[10] W. Luo, H.Y. Lan, Y. Xu et al., Implementation of the n-body Monte-Carlo event generator into the Geant4 toolkit for photonuclear studies. Nucl. Instrum. Meth. A **849**, 49–54 (2017). doi:10.1016/j.nima.2017.01.010
[11] S. Agostinelli, J. Allison, K. Amako et al., Geant4—a simulation toolkit. Nucl. Instrum. Meth. A **506**, 250–303 (2003). doi:10.1016/S0168-9002(03)01368-8
[12] Geant4. https://geant4.web.cern.ch/
[13] Q.H. Huang, D.H. Pan, Y.P. Xu et al., Application of the ^{68}Ge/^{68}Ga Generator in Clinic. Journal of Isotopes **30**, 270–275 (2017). doi:10.7538/tws.2017.youxian.024 **(in Chinese)**
[14] V.V. Varlamov, A.I. Davydov, M.A. Makarov et al., Reliability of the data on the cross sections of the partial photoneutron reaction for ^{63,65}Cu and ^{80}Se nuclei. Bull. Russ. Acad. Sci.: Phys. **80**, 317–324 (2016). doi:10.3103/S1062873816030333
[15] W. Luo, Production of medical radioisotope ^{64}Cu by photoneutron reaction using ELI-NP γ-ray beam. Nucl. Sci. Tech. **27**, 96 (2016). doi:10.1007/s41365-016-0094-6
[16] Y.C. Zhu, Q. Li, Y.Q. Fan et al., Establishment of Anti-cosmic Ray HPGe Gamma Spectrometer. Atomic Energy Science and Technology **57**(3), 639–645 (2023). doi:10.7538/yzk.2022.youxian.0243 **(in Chinese)**
[17] S.L. Zhou, Z.P. Luo, H.C. Pang et al., Study on the design of shielding of low-background anti-compton measurement system. Chin. J. Radiol. Health **27**, 562–566 (2018). doi:10.13491/j.issn.1004-714x.2018.06.012 **(in Chinese)**
[18] L.J. Diao, S.H. Yao, J. Meng et al., New anti-cosmic low-background γ-ray Spectrometer and its application. Paper presented at the Proceedings of the 15th National Nuclear Electronics and Nuclear Detection Technology Annual Conference, Guiyang, Guizhou, 13 Aug 2010.
[19] T.M. Semkow, P.P. Parekh, C.D. Schwenker et al., Low-background gamma spectrometry for environmental radioactivity. Appl. Radiat. Isotopes **57**, 213–223 (2002). doi:10.1016/S0969-8043(02)00085-4
[20] H.S. Miley, R.L. Brodzinski, J.H. Reeves, Low-background counting systems compared. J. Radioanal. Nucl. Ch. **160**, 371–385 (1992). doi:10.1007/BF02037112
[21] J.I. Byun, H.C. Yun, S.I. Kwak et al., An anticoincidence-shielded gamma-ray spectrometer for analysis of low level environmental radionuclides. Appl. Radiat. Isotopes **58**, 579–583 (2003). doi:10.1016/S0969-8043(03)00023-X

[22] L.J. Diao, T.Z. Hou, J. Meng et al., *in Annual Report of China Institute of Atomic Energy*, ed. by China Institute of Atomic Energy. 2019 Annual Conference of the Chinese Nuclear Society, Baotou, August 2019. Annual Report of China Institute of Atomic Energy. China Institute of Atomic Energy Annual Report 2019, (Atomic Energy Press, Beijing, 2019), p. 319

[23] G. Heusser, M. Weber, T. Denz et al., GIOVE, a shallow laboratory Ge-spectrometer with 100 μ Bq/kg sensitivity. AIP Conf. Proc. **1549**, 12–15 (2013). doi:10.1063/1.4818065

[24] G. Heusser, M. Weber, J. Hakenmüller et al., GIOVE: a new detector setup for high sensitivity germanium spectroscopy at shallow depth. Eur. Phys. J. C **75**, 531 (2015). doi:10.1140/epjc/s10052-015-3704-2

[25] Q.D. Hu, H. Ma, J.H. He et al., Design of cosmic veto shielding for HPGe-detector spectrometer. Appl. Radiat. Isotopes **109**, 474–478 (2016).

[26] H. Cheng, B.H. Sun, L.H. Zhu et al., Measurements of ^{160}Dy (p, γ) at Energies Relevant for the Astrophysical γ Process. Astrophy. J. **915**(2), 78 (2021). doi:10.3847/1538-4357/ac00b1

[27] J.W. Wang, G.T. Fan, H.W. Wang et al., Study on polarized γ beam properties of a new LCS light source based on SXFEL. Nucl. Techn. **42**, 120201 (2019). doi:10.11889/j.0253-3219.2019.hjs.42.120201 (in Chinese)

[28] K.J. Chen, L.X. Liu, Z.R. Hao et al., Simulation and test of the SLEGS TOF spectrometer at SSRF. Nucl. Sci. Tech. **34**, 47 (2023). doi:10.1007/s41365-023-01194-3

[29] L.C. He, L.J. Diao, B.H. Sun et al., Summing coincidence correction for γ-ray measurements using the HPGe detector with a low background shielding system. Nucl. I.nstrum Meth A **880**, 22–27 (2018). doi:10.1016/j.nima.2017.09.043

[30] X.D. Su, G.L. Zhang, S.P. Xu et al., Attenuation coefficients of gamma and X-rays passing through six materials. Nucl. Sci. Tech. **31**, 3 (2020). doi:10.1007/s41365-019-0717-9

[31] Y.H. Zuo, J.H. Zhu, P. Shang, Monte Carlo simulation of reflection effects of multi-element materials on gamma rays. Nucl. Sci. Tech. **32**, 10 (2021). doi:10.1007/s41365-020-00837-z

[32] M.J.M. Canet, M. Hult, M. KöhlerY et al., Measurements of activation induced by environmental neutrons using ultra low-level gamma-ray spectrometry. Appl. Radiat. Isotopes **52**(3), 711–716 (2000). doi:10.1016/s0969-8043(99)00234-1

[33] H.M. Portella, L.C.S.D. Oliveira, C.E.C. Lima et al., A new approach to derive atmospheric muon fluxes. J. Phys. G: Nucl. Part. Phys. **28**(3), 415–425 (2002). doi:10.1088/0954-3899/28/3/305

[34] W.N. Hess, H.W. Patterson, R. Wallace et al., Cosmic-Ray Neutron Energy Spectrum. Phys. Rev. **116**(2), 445–457 (1959). doi:10.1103/PhysRev.116.445

[35] D.K. Haines, T.M. Semkow, A.J. KhanD et al., Muon and neutron-induced background in gamma-ray spectrometry. Nucl. Instrum. Meth. A **652**(1), 326–329 (2011). doi:10.1016/j.nima.2011.01.137

[36] J.K. Yang, P.Q. Wang, Z.G. Ren et al., Comparison of neutron energy spectrum unfolding methods and evaluation of rationality criteria. Nucl. Sci. Tech. **33**, 164 (2022). doi:10.1007/s41365-022-01139-2

[37] T. Schroettner, M. Schwaiger, P. Kindl. Optimization of an active anti cosmic veto shielding. Appl. Radiat. Isotopes **61**(2/3), 133–138 (2004). doi:10.1016/j.apradiso.2004.03.034

[38] M.A. Lone, R.A. Leavitt, D.A. Harrison, Prompt gamma rays from thermal-neutron capture. Atom. Data Nucl. Data **26**(6), 511–559 (1981). doi:10.1016/0092-640X(81)90005-X

[39] A. Nachab, P. Hubert, ^{210}Pb activity by detection of bremsstrahlung in ^{210}Bi β-decay. Nucl. Instrum. Meth. B **274**, 188–190 (2012). doi:10.1016/j.nimb.2011.11.020

[40] F. Cannizzaro, M. Raneli, M.C. Spitale et al., Study of background characteristics of a low-level HPGe spectrometer with passive shielding in various configurations. Nucl. Instrum. Meth. A **390**(1/2), 167–174 (1997). doi:10.1016/S0168-9002(97)00313-6

[41] F. El-Daoushy, R. Garcia-Tenorio, Well Ge and semi-planar Ge (HP) detectors for low-level gamma-spectrometry. Nucl. Instrum. Meth. A **356**(2/3), 376–384 (1995). doi:10.1016/0168-9002(94)01351-9